

QCD MECHANISMS FOR HEAVY PARTICLE PRODUCTION \*

Stanley J. Brodsky  
Stanford Linear Accelerator Center, Stanford University,  
Stanford, California 94305

ABSTRACT

For very large pair mass, the production of heavy quarks and supersymmetric particles is expected to be governed by QCD fusion subprocesses. At lower mass scales other QCD mechanisms such as prebinding distortion and intrinsic heavy particle Fock states can become important, possibly accounting for the anomalies observed for charm hadroproduction. We emphasize the importance of final-state Coulomb interactions at low relative velocity in QCD and predict the existence of heavy narrow four quark resonances ( $c\bar{c}u\bar{u}$ ) and ( $c\bar{c}\bar{c}$ ) in  $\gamma\gamma$  reactions. Coherent QCD contributions are discussed as a contribution to the non-additivity of nuclear structure functions and heavy particle production cross sections. We also predict a new type of amplitude zero for exclusive heavy meson pair production which follows from the tree-graph structure of QCD.

1. Introduction

The central focus of the physics of new colliders will be the production of new quark flavors, supersymmetric particles, and other systems coupling to color in quantum chromodynamics. For very large pair mass, the hadronic production of heavy quarks and supersymmetric particles is expected to be governed by QCD fusion subprocesses,  $gg \rightarrow Q\bar{Q}$  and  $q\bar{q} \rightarrow Q\bar{Q}$ . In addition, there are interesting QCD mechanisms which, though power law suppressed relative to the fusion contribution, may play a major role in charm and possibly beauty production. These new mechanisms can also lead to observable novel effects for  $t\bar{t}$  production. A full understanding of the QCD predictions is needed to project rates for supersymmetric and other new particles, as well as to understand backgrounds to other rare processes.

The experimental situation for the hadroproduction of charm is now particularly intriguing—virtually none of the expectations predicted by the fusion mechanisms seem to be seen in the data: the cross sections at the ISR are larger than predicted and much flatter at large longitudinal momentum fraction  $x_L$  than expected from gluon distributions.<sup>1-4</sup> Recent measurements at Fermilab<sup>5</sup> indicate that the cross section for charm production by 400 GeV protons on nuclear targets varies as  $A^\alpha$  where  $\alpha = 0.75 \pm 0.05$ , contrary to the linear  $A^1$  dependence on nucleon number expected from perturbative QCD mechanisms. Measurements<sup>6</sup> of the cross section  $\Sigma^- N \rightarrow A^+(csu) + X$  indicate that production of charm by hyperons is much larger than that for proton beams, contrary to the beam flavor-independence expected from fusion mechanisms. There are also experimental indications from the EMC deep inelastic muon scattering experiment<sup>7</sup> that the charm contribution to the proton structure

\* Work supported by the Department of Energy, contract DE - AC03 - 76SF00515.

functions could be considerably larger at large  $W^2$  and  $x_{Bj}$  than expected from perturbative evolution (photon-gluon fusion). Finally, as reported by the UA1 group<sup>8</sup> the number of charged  $D_{\pm}^*$  per high  $p_T^{jet}$  at the  $Spp\bar{S}$  collider appears to be significantly larger than predicted from perturbative processes.

All of these anomalies suggest new dynamical mechanisms for heavy particle production and offer the opportunity to obtain new insights into the basic mechanisms for hadroproduction in QCD.

## 2. Charm Hadroproduction

An extensive review of the measurements of charm production in hadron collisions has now been published so the discussion here will be relatively brief.<sup>2,3</sup> The first experiments at the ISR indicated that the total charm production cross section is of the order of 1 mb at  $\sqrt{s} = 53$  to 63 GeV. Compatibility with the latest  $D$  branching ratios and the measured  $e/\pi$  ratio (extrapolated from data in the central rapidity region) implies<sup>2</sup> a somewhat smaller cross section:  $\sigma(D\bar{D} + X) \leq 500\mu b$  and  $\sigma(\Lambda_c\bar{D} + X) \leq 100\mu b$  at  $\sqrt{s} = 62$  GeV. (See Figure 1). A recent analysis<sup>9</sup> of so-called "long-flying" cascades in cosmic ray data at lab energies above 40 TeV ( $\sqrt{s} \gtrsim 300$  GeV) suggests heavy quark production cross sections of order  $4 \pm 1$  mb/nucleon. The fusion subprocesses predict charm cross sections of order  $100\mu b$  or less at ISR energies.

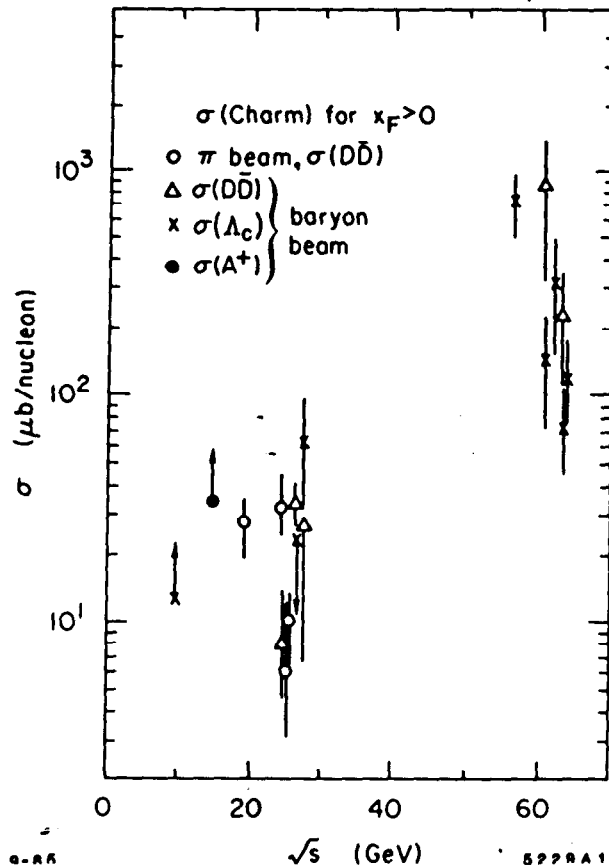


Figure 1: Compilation of charm hadroproduction data, from Ref. 4.

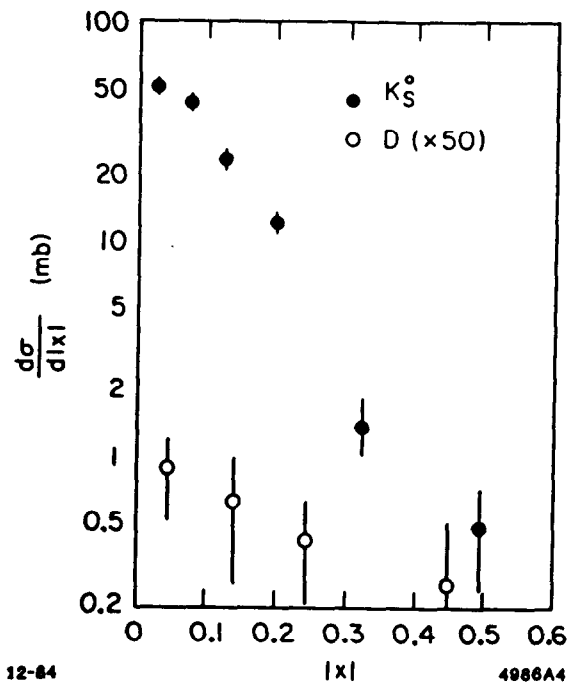


Figure 2: Comparison of kaon and  $D$  meson production in  $pp$  collisions. From S. Reucroft, Ref. 11.

The ISR data implies nearly flat production of charm hadrons at large  $x_L$ , particularly  $\Lambda_c$  production:<sup>10</sup>  $d\sigma/dx_L (pp \rightarrow \Lambda_c X) \sim (1 - x_L)^{0.40 \pm 0.25}$ , including possible contributions from the diffractive process  $pp \rightarrow p\Lambda_c X$ . At SPS-FNAL energies ( $19 < \sqrt{s} < 26 \text{ GeV}$ ) charm production cross sections are apparently an order of magnitude smaller, but still indicate relatively fast forward charm hadron production; the LEBC-EHS hydrogen bubble chamber experiment<sup>11</sup> ( $pp$  collisions at  $E_{\text{lab}} = 360 \text{ GeV}$ ), which has relatively flat acceptance in  $x_L$  finds  $dN/dx_L \sim (1 - x_L)^{1.8 \pm 0.8}$  for the production of  $D^+(c\bar{d})$ ,  $D^-(\bar{c}d)$ ,  $D^0(c\bar{u})$ , and  $\bar{D}^0(\bar{c}u)$  independent of whether the  $D$  or  $\bar{D}$  carries a valence quark of the proton or not. The corresponding strange-particle production cross section is much steeper (see Fig. 2). Although statistically weak, the LEBC results suggest that the charm quark momentum distributions probed in proton collisions are much harder than those for strange quarks. This disparity is clearly difficult to explain in terms of the  $gg \rightarrow c\bar{c}$  fusion mechanism. The E613<sup>12</sup> and E595<sup>13</sup> Beam Dump experiments at FNAL report a steeper distribution  $(1 - x)^{5 \pm 1}$  for  $D$ 's produced in tungsten and iron targets, but this result could be compatible with the LEBC experiment if the nuclear target dependence is strongly dependent on  $x_L$ , which is generally the case for soft hadron production.<sup>14</sup> The only explicit  $A$ -dependent measurement, the Michigan Beam Dump experiment<sup>3</sup> (400 GeV  $p \text{ Be}$ ,  $p \text{ W}$  collisions), indeed indicates a nontrivial  $A$ -dependence. (See Figure 3.)

Another intriguing anomaly in charm hadroproduction is seen in the WA-42 experiment<sup>6</sup> at the SPS, which reports copious production of the  $A^+(csu)$  charmed strange baryon in 135 GeV  $\Sigma^-$  collisions on a beryllium target. The  $A^+$  is observed in the  $\Lambda K^- \pi^+ \pi^+$

channel with a hard distribution  $(1 - x_L)^{1.7 \pm 0.7}$  for  $x_L > 0.6$ . The corresponding cross section times branching ratio (taking the above form for all  $x_L$ ), for forward  $x_L$  is  $4.7 \mu\text{b}/\text{nucleon}$  assuming  $A^1$  dependence. If the branching ratio for the measured channel is 3% to 5% this implies a total cross section in the 100 to 150  $\mu\text{b}$  range, compared to cross sections of order 30  $\mu\text{b}$  for  $pp \rightarrow \Lambda_c X$  measured at higher energies in the LEBC experiment. Even larger cross sections would be expected for charmed-strange ( $csd$ ) baryons which carry two valence quarks of the  $\Sigma^-(sdd)$ . The experimental results suggest the possibility of systematically enhanced production of heavy quark states by hyperon and kaon beams.

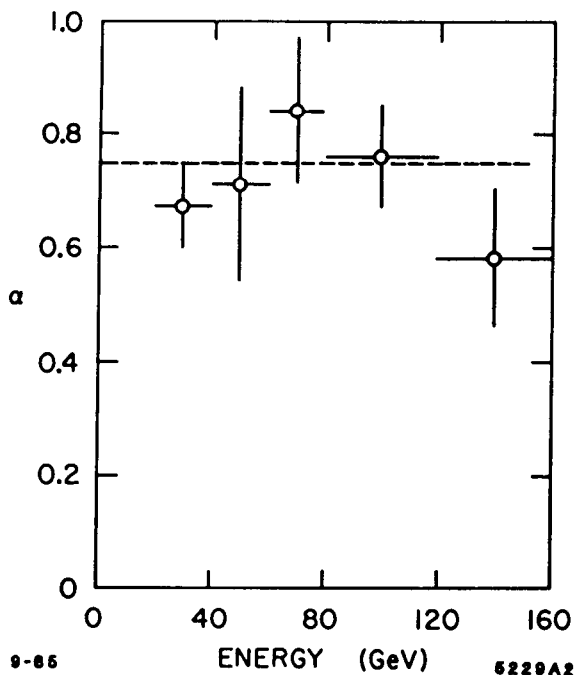


Figure 3: Nuclear number  $A^\alpha$  dependence of the charm cross section as a function of neutrino energy.<sup>3</sup>

Since the momentum of a charmed hadron tends to follow the momentum of the produced charmed quark (the Bjorken-Suzuki effect), the hadroproduction data indicates that charm quarks have large momentum fraction in the nucleon more characteristic of a valence quark than a sea quark distribution. This question can be settled directly by measurements of deep inelastic scattering of leptons on the charm constituents of the nucleon at  $Q^2 \gg 4m_c^2$ . The available high  $Q^2$  data from the EMC collaboration<sup>7</sup> (see Fig. 4), as extracted from  $\mu N \rightarrow \mu\mu X$  data, indeed does seem to indicate an anomalously large  $c(x, Q^2)$  distribution at large  $Q^2$  and  $x_{Bj} \sim 0.4$  compared to that expected<sup>1,15</sup> for the photon-gluon fusion diagrams or equivalently, from QCD evolution. Although the data has low statistics and thus could be misleading, it clearly suggests the existence of mechanisms for charm production other than the standard photon-gluon fusion subprocess. In this talk we will discuss two interrelated effects which are in the direction to enhance charm production at large  $x_L$  and are surely present in QCD at some level. Much more theoretical and experimental work will be required to verify whether these effects can account for the observed features

of heavy quark hadroproduction.

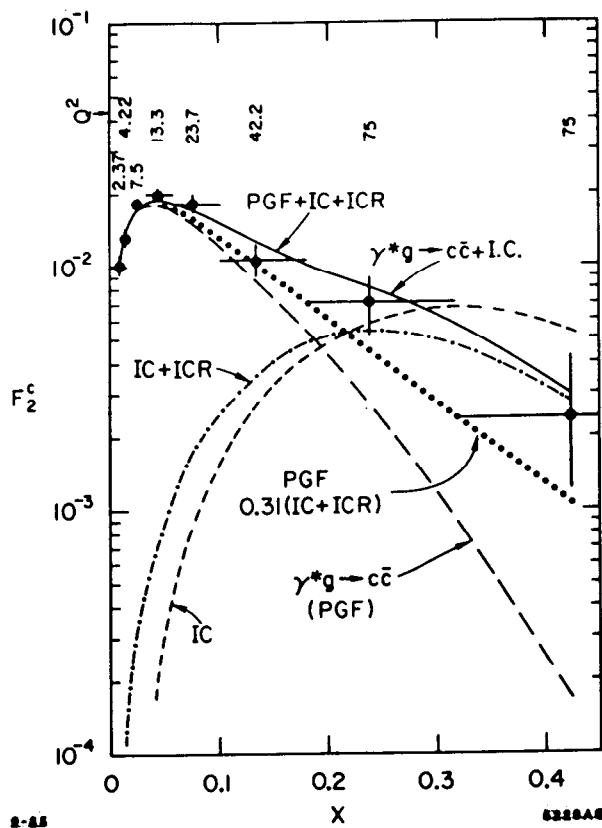


Figure 4: Analysis of the charm structure function of the proton by Hoffmann and Moore,<sup>15</sup> in terms of PGF (photon-gluon fusion  $\gamma^* g \rightarrow c\bar{c}$ ), IC (1% intrinsic charm), and ICR (radiated intrinsic charm components). The data are from the EMC collaboration.

### 3. Validity of the Fusion Mechanism in QCD

Although there is no systematic all-orders proof of the validity of the fusion mechanism as the dominant production process for heavy particles in QCD, a recent perturbative analysis by Collins, Soper and Sternman<sup>16</sup> suggests that the basic factorization formalism is valid to leading order in  $1/M_Q^2$ .

There are several experimental conditions necessary for the validity of the analysis.

1. As was shown<sup>17</sup> first for the Drell-Yan process, the active parton energy must be large compared to a scale proportional to the length of the target:

$$x_a s > M_N^2 L_A \mu^2 \quad (3.1)$$

where  $\mu^2$  is a typical hadron scale and  $L_A$  is the length of the target in its rest frame.

2. The transverse momenta  $p_T^c$  and  $p_T^d$  of the produced heavy particles must be of order  $M_Q$  (the natural scale).
3. The rapidity difference  $y_c - y_d$  must be finite.
4. The production energy must be well above threshold,  $s \gg 4m_Q^2$ .

The leading order analysis of CSS then indicates that the fusion  $gg \rightarrow Q\bar{Q}$  and  $q\bar{q} \rightarrow Q\bar{Q}$  subprocesses and the factorization formula

$$\frac{d\sigma}{dx_a dx_b} = \sum_{ab} \int_0^1 dx_a \int_0^1 dx_b G_{a/A}(x_a, Q) G_{b/B}(x_b, Q) \sigma_{ab \rightarrow cd}(x_a x_b s) \quad (3.2)$$

is correct to leading order in  $\mu^2/m_Q^2$  and  $\alpha_s(m_Q^2)$ . The formal, gauge invariant, definition of the gluon distribution in a hadron is

$$F.T. \langle p | F_a^{\mu\nu}(y^+, y^- = 0, y_\perp = 0) \left( P \exp ig \int_0^{y^+} dz A_b^+ T_b \right) F_{\mu\nu}^a(0) | p \rangle \quad (3.3)$$

which reduces to the usual Fock state probability sum in  $A^+ = 0$  gauge.<sup>18</sup> The analysis of CSS also shows that diffractive-type diagrams are already included in Eqs. (3.2) and (3.3) to leading order and should not be added separately.

As yet the  $K$  factors from higher order radiative corrections  $\sim (1 + C_1 \pi \alpha_s(m_Q^2))$  appropriate to fusion subprocesses have not been evaluated. Because of the larger color factors, the  $\pi \alpha_s$  correction to  $gg \rightarrow Q\bar{Q}$  could be significantly larger than the corresponding  $K$ -factor for the Drell-Yan process.

Physically, factorization is expected to be valid when initial and final state interactions with the spectator constituents of the incident and outgoing hadrons can be neglected.<sup>19</sup> The basic fusion production process occurs within a "unitary volume"  $\Delta b_\perp \Delta z$  where (in the target rest frame)

$$\Delta b_\perp \sim (p_T^Q)^{-1}, \quad \Delta z \sim (m_Q v_Q)^{-1}.$$

Only gluons with wavelength sufficiently short relative to the unitary volume can resolve the produced pairs and cause significant reinteractions with the spectator hadrons. Thus breakdown of factorization can occur when  $k_\perp \sim O(p_\perp^Q)$  or  $k_z \sim O(m_Q v_Q)$ ; *i.e.*, important final state corrections to the QCD factorization formula may occur when the heavy pair is produced at low  $p_T$  or at small relative rapidity in the target (or beam) fragmentation regions. Such behavior is well known in QED, which predicts a strong redistribution of the basic Bethe-Heitler Born amplitude for pair production in the Coulomb field of the target. We discuss this further in the next section.

#### 4. Distortion Due to Pre-binding Effects in Heavy Quark Production

Although the fusion subprocess  $gg \rightarrow Q\bar{Q}$  is evidently the dominant mechanism for  $t$ -quark production in high energy  $pp$  collisions, it is not clear that the application of QCD perturbation theory (*i.e.* Born approximation) to the total production cross section in all kinematic regions is justified. As an example of the types of complications possible, consider the cross section for the photoproduction of a heavy lepton pair in the Coulomb field of a nucleus in QED. For large  $Z$  the cross section is strongly distorted at slow lepton velocities  $v_\pm \ll Z\alpha$  by multiple soft Coulomb interactions<sup>20</sup>

$$d\sigma(\gamma Z \rightarrow \ell\bar{\ell}X) = d\sigma_0 \frac{s_+ s_-}{(e^{s_+} - 1)(1 - e^{-s_-})}. \quad (4.1)$$

Here  $d\sigma_0$  is the Bethe-Heitler cross section computed in Born approximation, and

$$\zeta_+ = \frac{2\pi Z\alpha}{v^+}, \quad \zeta_- = \frac{2\pi Z\alpha}{v^-}. \quad (4.2)$$

These results are strictly valid for  $\zeta_+ \ll 1$ , but  $\zeta_-$  can be unrestricted. The effect of the correction factor is to distort the cross section toward small negative-lepton velocity (relative to the target rest frame). As  $v^- \Rightarrow 0$ , the enhancement is so strong that even the threshold phase-space suppression factor in  $\sigma_0$  is cancelled. Conversely, the cross section is exponentially damped when the positive lepton has low velocity.

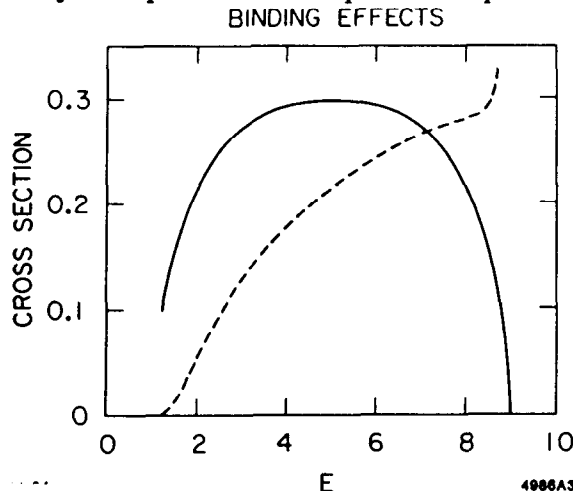


Figure 5: The Bethe-Heitler cross section  $\gamma Z \rightarrow \ell^+ \ell^- Z$  in Born approximation as a function of the positive lepton energy. The dotted curve shows the modified spectrum due to multiple scattering using Eq. (4.1) with  $Z\alpha \rightarrow 4/3 \alpha_s(Q^2)$ . We have used  $\alpha_s(Q^2) = 4\pi/(\beta_0 \ln(1 + Q^2/\Lambda^2))$ ,  $|\alpha_s| < 4$ , where  $\Lambda = 200$  MeV and  $Q^2$  is the 4-momentum squared of the lepton relative to the target.

An analogous effect evidently will also occur in QCD.<sup>21</sup> For example in charm photoproduction  $\gamma p \rightarrow c\bar{c}X$ , we expect the Born cross section based on photon-gluon fusion  $\gamma g \rightarrow c\bar{c}$  to be strongly distorted toward charm production in the target fragmentation region; e.g. the charm quark rapidity will be skewed toward that of the spectator  $qq$  system of the nucleon where it can bind to form color singlets. As a simple model we will estimate<sup>21</sup> this prebinding effect by replacing  $\pi Z\alpha \rightarrow \frac{4}{3} \pi \alpha_s(Q^2)$  in the QED distortion factor, Eq. (4.1). (We take  $Q^2$  to be the relative momentum of the  $c$ -quark and the spectator system and limit  $|\alpha_s| \leq 4$ .) Clearly this gives only a very rough estimate of physics controlled by QCD non-perturbative effects. As shown in Fig. 5, the behavior predicted by this model indicates significant increases in the magnitude of the heavy quark production cross sections and significant skewing of the heavy particle momentum distribution towards large  $x_L$ . We are presently exploring further predictions of this model, including the effects of recombination with the incident valence quarks and the influence of strange quarks in the beam.

It thus seems likely that the distortion of the fusion Born approximation cross section due to prebinding attractive forces in QCD will be significant for the production of heavy quarks at collider energies, enhancing the production of  $\Lambda_c, \Lambda_b, \Lambda_t$ , etc. in the forward region. Unlike the case of final-state interaction corrections to hard scattering

processes, the corrections discussed here coherently enhance the production process and are not limited by unitarity to be of  $\mathcal{O}(1)$ . If there are strange quarks in the incident-hadron, then the distortion is likely to be magnified, since a strange quark tends to be more non-relativistic than  $u$  and  $d$  quarks in a hadron and thus more effective in "capturing" other quarks. This possibility could explain the relatively copious production of the  $A^+(csu)$  in the  $\Sigma^-$  fragmentation region, and suggests an important role of hyperon and strange meson beams for charm and heavy particle production experiments.

The nominal scaling behavior for the total heavy quark production cross section based on the  $gg \rightarrow Q\bar{Q}$  process is

$$\sigma_{Q\bar{Q}}(\sqrt{s}) = \frac{m_c^2}{m_Q^2} \sigma_{c\bar{c}} \left( \sqrt{s} = \frac{m_c}{m_Q} \sqrt{s} \right). \quad (4.3)$$

The prebinding distortion factor is not expected to significantly modify this behavior. Assuming that most of the observed charm cross section is non-intrinsic we may use Eq. (4.3) to extrapolate to the heavier quarks. For production well above threshold ( $s \gg 4m_Q^2$ ), the  $\frac{1}{2} mb$  charm cross section reported at the ISR implies  $\sigma_{b\bar{b}} \sim 50 \mu b$  at the  $SP\bar{P}S$  collider ( $\sqrt{s} = 540$  GeV) and  $\sigma_{t\bar{t}} \sim \frac{1}{2} \mu b$  at the SSC ( $\sqrt{s} = 40$  GeV).

At lower energies we can extrapolate the  $\sim 20 \mu b$  charm cross section at SPS/FNAL energies ( $\sqrt{s} \cong 20$  GeV) using

$$\frac{m_c = 1.8 \text{ GeV}}{\sqrt{s} = 20 \text{ GeV}} \cong \frac{m_b = 5 \text{ GeV}}{\sqrt{s} = 63 \text{ GeV}} \cong \frac{m_t = 40 \text{ GeV}}{\sqrt{s} = 540 \text{ GeV}} \quad (4.4)$$

to obtain  $\sigma_{b\bar{b}}(\sqrt{s} = 63 \text{ GeV}) \sim 2 \mu b$  at the ISR and  $\sigma_{t\bar{t}}(\sqrt{s} = 540 \text{ GeV}) \sim 20 \mu b$  at the  $SP\bar{P}S$  collider. We predict a sizeable fraction of these events to be diffractive in nature, producing high- $x_L$   $b\bar{b}$  or  $t\bar{t}$  heavy quark systems. This extrapolation also predicts

$$\sigma_{Q\bar{Q}}(m_Q = 1 \text{ TeV}, \sqrt{s} = 40 \text{ TeV}) \sim 10^{-3} \mu b. \quad (4.5)$$

Similar extrapolations are of interest for hyperon beams. Extrapolating from the WA42 experiment at  $\sqrt{s} = 16$  GeV we predict

$$B\sigma(\Sigma^- N \rightarrow \Sigma^0(bsu)X) \sim 1 \mu b \quad (4.6)$$

at  $\sqrt{s} \sim 50$  GeV, assuming that the branching ratio for the  $\Sigma^0(bsu)$  decay channel is similar to that for the  $\Lambda K^- \pi^+ \pi^+$  channel in which  $A^+(csu)$  is seen by WA42.

Bjorken<sup>22</sup> has extrapolated present hadroproduction data to the case of heavy baryon production with two or more heavy quarks  $|css\rangle, |ccs\rangle, |ccc\rangle$ , etc. (See Table I). Note the factor of 20 increase from nucleon to hyperon-induced cross sections.

Table I  
 $\sigma(\sqrt{s} = 40 \text{ GeV}, x \geq 0.4)$

Beam:	$n, p$	$\pi$	$\Sigma^-$	$K^-$
$ csu\rangle$	$2.5 \mu\text{b}$	$500 \text{ nb}$	$50 \mu\text{b}$	$5 \mu\text{b}$
$ css\rangle$	$100 \text{ nb}$	$50 \text{ nb}$	$2 \mu\text{b}$	$500 \text{ nb}$
$ ccd\rangle$	$10 \text{ nb}$	$20 \text{ nb}$		
$ ccs\rangle$	$500 \text{ pb}$	$500 \text{ pb}$	$10 \text{ nb}$	$5 \text{ nb}$
$ ccc\rangle$	$3 \text{ pb}$	$10 \text{ pb}$	$3 \text{ pb}$	$10 \text{ pb}$

### 5. Intrinsic Heavy Quark Fock States

In a relativistic quantum field theory, a bound state cannot be described in terms of a fixed number of constituents at a given time, since Fock states beyond the minimal valence component are always generated from exchange forces. For example, at fixed time on the light-cone  $\tau = t + z$ , the probability of non-valence states in a state of mass  $M$  is given by  $\langle \partial V_{\text{eff}} / \partial M^2 \rangle$  where  $V_{\text{eff}}$  is the effective potential constructed from the light-cone Hamiltonian truncated onto the valence Fock state sector.<sup>18</sup> Thus, positronium in QED at equal time on the light-cone contains a spectrum of Fock states  $|e^+e^- \rangle$ ,  $|e^+e^-\gamma \rangle$ ,  $|e^+e^-e^+e^- \rangle$ ,  $|e^+e^-\mu^+\mu^- \rangle$ , etc. generated from (non-instantaneous) photon exchange, vacuum polarization, light-by-light insertions, etc. At equal  $\tau$  the constituents  $i = 1, \dots, n$  in each Fock state  $\psi_n$  are on their mass shells:  $k_i^2 = m_i^2$ ,  $k^0 > 0$ , satisfy 3-momentum conservation:  $\sum_{i=1}^n \vec{k}_{\perp i} = \vec{p}_{\perp} = 0$ ,  $\sum_{i=1}^n x_i = 1$  ( $x_i \equiv k_i^+ / P^+$ ,  $0 < x_i < 1$ ), but are off the light-cone energy shell:  $\epsilon_n \equiv M^2 - \sum_i [(k_{\perp i}^2 + m_i^2) / x_i] < 0$ . The structure function and momentum distributions of the constituents at resolution scale  $Q$  can be computed directly from the light-cone wavefunctions summed over all Fock states:

$$G_{a/p}(x, Q) = \frac{dN}{dx} = \sum_n \int_{k_{\perp}^2 < Q^2} [d^2 k_{\perp}] [dx] \sum_{i=a} \delta(x_i - x) |\psi_n(x_i, \vec{k}_{\perp i})|^2. \quad (5.1)$$

Thus, in the case of positronium, a finite fraction of its momentum ( $\mathcal{O}(1/m_{\mu}^2)$ ) is carried by muon constituents [at resolution scales  $Q^2 \gtrsim \mathcal{O}(m_{\mu}^2)$ ]. The momentum distributions of the intrinsic heavy constituents reflect the light-cone energy denominator

$$\frac{dN}{d^2 k_{\perp} dx} \sim \left[ \frac{\Gamma(x)}{M^2 - \sum_{i=1}^n \left( \frac{k_{\perp i}^2 + m_i^2}{x} \right)} \right]^2 \quad (5.2)$$

which tends to peak at  $x_i \propto \sqrt{m_i^2 + k_{\perp i}^2}$ , i.e. equal rapidity or relative velocity of the constituents. This effect has been worked out in QED by K. Hornbostel<sup>22</sup> who finds that the momentum distribution of a muon in the positronium  $|e^+e^-\mu^+\mu^- \rangle$  Fock state indeed tends to significantly broaden to large  $x$  as the binding energy is increased so that momentum can be readily transferred from the valence ( $e^+e^-$ ) to heavy

$(\mu^+ \mu^-)$  constituents. The contribution of the heavy-pair vacuum polarization to the photon wavefunction renormalization corresponds to the standard sea or “extrinsic” contribution induced by QCD evolution.

It is thus natural to look at the role of intrinsic heavy quark Fock states in the nucleon bound state wavefunction in QCD.<sup>24</sup> To leading order in  $1/m_Q^2$  the intrinsic contributions correspond to twist six terms in the effective QCD Lagrangian<sup>16</sup>

$$\begin{aligned} \mathcal{L}_{QCD}^{eff} = & -\frac{1}{4} F_{\mu\nu a} F^{\mu\nu a} - \frac{g^2 \frac{N_C}{2}}{60\pi^2 m_Q^2} D_\alpha F_{\mu\nu a} D^\alpha F^{\mu\nu a} \\ & + C \frac{g^3}{\pi^2 m_Q^2} F_\mu^{a\nu} F_\nu^{b\tau} F_\tau^{c\mu} f_{abc} + \mathcal{O}\left(\frac{1}{m_Q^4}\right). \end{aligned} \quad (5.3)$$

For QED  $e^2(\partial_\alpha F_{\mu\nu})^2/60\pi^2 m_l^2$  gives the standard Serber-Uehling vacuum polarization contribution to the mass shift of an atom due to heavy lepton pairs. In QCD the corresponding  $\alpha_s(D_\alpha F_{\mu\nu})^2/m_Q^2$  term yields a heavy quark pair contribution with probability of order  $1/m_Q^2$  in the proton state with from two to six gluon attachments to the nucleon constituents. As in the atomic case, the running coupling constant  $\alpha_s(k^2)$  is evaluated at the soft momentum scale of the bound state, not at the heavy particle mass scale. Since the coupling constant is large and there are many contributing graphs, it is not unreasonable that the momentum carried by a charm quark pair in the nucleon is of the order of 1/3%, as indicated by the EMC data.<sup>7</sup> (See Fig. 4).

In addition to causing a shift in the nucleon mass, the dimension-six contributions of the effective Lagrangian imply the existence of Fock states in the nucleon containing an extra  $Q\bar{Q}$  pair. Lattice gauge theory or the light-cone equation of state could determine the hadronic wavefunctions and determine the heavy particle content. At this time we can deduce<sup>24,25</sup> the following semiquantitative properties for intrinsic states such as  $|uudQ\bar{Q}\rangle$ :

1. The probability of such states in the nucleon is nonzero and scales as  $m_Q^{-2}$ .
2. The maximal wavefunction configurations tend to have minimum off-shell energy, corresponding to constituents of equal velocity or rapidity, *i.e.*,

$$x_i \equiv \frac{(k^0 + k^z)_i}{p^0 + p^z} \propto \sqrt{(k_\perp^2 + m^2)_i}. \quad (5.4)$$

Thus the heavy quarks tend to have the largest momentum fraction in the proton wavefunction, just opposite to the usual configuration assumed for sea quarks.

3. The transverse momenta of the heavy quarks are roughly equal and opposite and of order  $m_Q$ , whereas the light quarks tend to have soft momenta as set by the hadron wavefunction.
4. The effects are strongly dependent on the features of the valence wavefunction: the intrinsic heavy quark probability is thus presumably larger in baryons than

in mesons, non-additive in nucleon number in heavy nuclei, and sensitive to the presence of strange quarks.

5. In deep-inelastic scattering on an intrinsic charm quark the heavy quark spectator will be found predominately in the target fragmentation region.

The charm structure function does not become fully observable unless the available energy is well above threshold:  $W = (q + p)^2 \gg W_{th}^2 = 4m_Q^2$ . The correct rescaling variable for deep inelastic muon scattering is roughly  $x = x_{Bj} + W_{th}^2/W^2$ , not  $x = x_{Bj} + m_Q^2/Q^2$  which is appropriate charge-current single heavy quark excitation.

The presence of intrinsic charm quarks in the nucleon also has implications for other hard scattering processes involving incident charmed quarks. In general, the charm quark in the nucleon will reflect both extrinsic and intrinsic ( $1/m_c^2$ ) contributions. Using QCD factorization this implies significant intrinsic charm contributions to hard scattering processes such as  $c + g \rightarrow c + X$  at  $p_T^2 \gg 4m_c^2$ , with the intrinsic contribution dominating the large  $x$  domain. The characteristic signal for such contributions is a  $\bar{c}$  spectator jet in the beam fragmentation region. These hard-scattering results can also be applied to  $b$ -quark and  $t$ -quark production processes, with the intrinsic structure function scaling as  $1/m_Q^2$  for  $p_T^2 \gg 4m_Q^2$  at production energies well above threshold. Similarly, if supersymmetric particles of mass  $\tilde{m}$  exist, they contribute to intrinsic SUSY Fock states<sup>25</sup> in the nucleon at order  $1/\tilde{m}^2$ . The intrinsic  $\tilde{q}(x)$  or  $\tilde{g}(x)$  distribution is again predicted to dominate at large  $x$ . Hard scattering processes such as  $\tilde{q} + \bar{q} \rightarrow \tilde{\gamma} + \gamma$  can produce purely electromagnetic monojet events. Note that the associated supersymmetric  $\tilde{\tilde{q}}$  or  $\tilde{\tilde{g}}$  partner appears in the beam fragmentation region.

The presence of a hard-valence-like charm distribution in the nucleon can, at least qualitatively, explain some of the anomalous features of the charm hadroproduction data discussed.<sup>24</sup> The fact that the  $c$  and  $\bar{c}$  as well as  $D$  and  $\bar{D}$  distributions are harder than the corresponding strange particle distributions can be attributed to the fact that the skewing of quark distributions to large  $x$  only really becomes effective for quarks heavier than the average momentum scale in the nucleon. One can explain the nearly flat  $\Lambda_c$  cross section if there is recombination of the intrinsic charm quarks with the  $u$  and  $d$  spectator quarks of the nucleon. We note that recombination itself cannot explain the comparable distributions observed in the LEBC experiment for  $D$  and  $\bar{D}$ , unless it is the heavy quarks that carry most of the momentum. Thus diffractive excitation of the intrinsic heavy quark Fock states may well be the source of the relatively large diffractive cross section  $pp \rightarrow \Lambda_c \bar{D} X$  indicated by ISR measurements.

A crucial question is the extrapolation of the intrinsic heavy quark contribution to  $b$  and  $t$  quarks. The fusion cross section scales as  $1/m_Q^2$ . As shown in Ref. 26, the intrinsic contribution actually scales as  $1/m_Q^4$  at high energies since the probe momentum must be sufficiently large ( $|t| > m_Q^2$ ) in order to unveil the intrinsic  $1/m_Q^2$  scaling Fock states. This is contrary to the expectations stated in Refs. 24-25. Thus it seems unlikely that the intrinsic contribution will be more important than the fusion process  $gg \rightarrow Q\bar{Q}$  for the total  $t$ -quark hadroproduction.

## 6. Heavy Flavors form Gluon Jets

It is straightforward to predict the heavy quark content of a gluon jet from perturbative QCD. The basic  $g \rightarrow Q\bar{Q}$  tree graph gives the distribution

$$\frac{dN}{dx dk_{\perp}^2} = \frac{\alpha_s}{4\pi} \left\{ \frac{k_{\perp}^2 (x^2 + (1-x)^2) + \frac{1}{2}m_Q^2}{(k_{\perp}^2 + m_Q^2)^2} \right\}$$

where  $x = (k_Q^0 + k_{\bar{Q}}^z)/(p_g^0 + p_g^z)$  is the light-cone momentum fraction and  $M^2 = (k_{\perp}^2 + m_Q^2)/x(1-x)$  is the invariant pair mass. The  $\frac{1}{2}m_Q^2$  term corresponds to the case of parallel  $Q\bar{Q}$  helicities. Integrating over  $0 < x < 1$  gives<sup>27</sup>

$$\frac{dN}{dM^2} = \frac{\alpha_s(M^2)}{6\pi M^2} \sqrt{1 - \frac{4m_Q^2}{M^2}} \left[ 1 + \frac{2m_Q^2}{M^2} \right].$$

The number of pairs per gluon jet at the virtuality scale  $Q^2$  is then

$$\rho(Q^2) = \int_{4m_Q^2}^{Q^2} \frac{dM^2}{M^2} \alpha_s(M^2) \left[ 1 + \frac{2m_Q^2}{M^2} \right] \sqrt{1 - \frac{4m_Q^2}{M^2}} n_G(Q^2, M^2)$$

where  $n_g(Q^2, M^2)$  is the number of gluon jets of virtuality  $M^2$  at the scale  $Q^2$  [see Ref. 28]. The result has a different shape and is significantly below the rate of charged  $D^*$  reported by the UA1 group. Recently, Mueller and Nason<sup>29</sup> have computed the non-perturbative contribution to  $\rho(Q^2)$  due to a non-zero vacuum condensate for  $\alpha_s F_{\mu\nu}^2$ . The result is

$$\begin{aligned} \rho_{\text{non-pert}} &= \frac{\langle \Omega | F_{\mu\nu}^2 \alpha_s | \Omega \rangle}{m_Q^4} \frac{\alpha_s(m_Q^2)}{(N_c^2 - 1)} \left( -\frac{C_F}{30} + \frac{53}{3780} C_A \right) \\ &\cong -2.2 \times 10^{-6} \alpha_s(m_c), \end{aligned}$$

which is negligible compared to the perturbative contribution.

## 7. Heavy Four-quark state production in $\gamma\gamma$ collisions

In photon-photon collisions each photon will preferentially couple to a charge 2/3 quark as indicated in figure (6). This implies the production of  $u\bar{u}u\bar{u}$ ,  $u\bar{u}c\bar{c}$ , and  $c\bar{c}c\bar{c}$  states. The one-gluon exchange cross section is of order

$$\sigma_{\gamma\gamma \rightarrow q_a \bar{q}_a q_b \bar{q}_b} \sim \frac{e_a^2 e_b^2 \alpha^2 \alpha_s^2 (M^2)}{\pi M^2}$$

where  $M$  is the heavier of  $m_a$  and  $m_b$ .

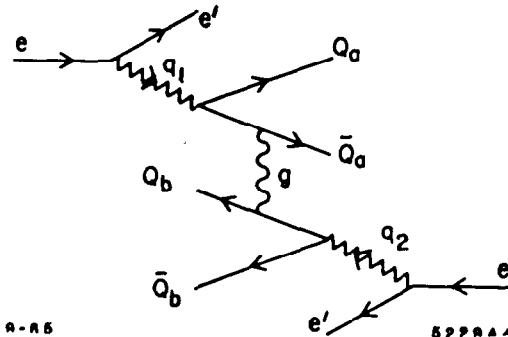


Figure 6: Tree diagram for four quark production in photon-photon collisions.

Just as in the case of the Schwinger correction to  $\sigma(e^+e^- \rightarrow q\bar{q})$  there are large radiative corrections of order  $\frac{\pi\alpha_s}{\beta}$  from final state Coulomb interactions which cancel the phase-space suppression at threshold. This strong effect at threshold reflects the breakdown of perturbation theory due to the strong attraction of the  $(q\bar{q})_8$  and  $(q\bar{q})_8$  pairs in the final state. As in the case of charmonium resonances in  $e^+e^-$  annihilation, one expects significant resonant  $|u\bar{u}c\bar{c}\rangle$  and  $|c\bar{c}c\bar{c}\rangle$  near 3 and 6 GeV. Such exotic states could be very narrow. Important decay channels are likely to be  $\gamma + \bar{D}D$ , and hadrons  $+ D\bar{D}$ . If such states are found, it would be conclusive evidence of the role QCD exotics in the hadronic spectrum and it would lend support to the hypothesis that  $|qq\bar{q}\bar{q}\rangle$  states are the origin of the large cross sections seen in  $\gamma\gamma \rightarrow \rho^0\rho^0$ . We also expect anomalous resonances to show up in  $\gamma\gamma \rightarrow s\bar{s}s\bar{s}$ ,  $s\bar{s}c\bar{c}$ ,  $c\bar{c}b\bar{b}$ ,  $b\bar{b}b\bar{b}$ , etc., although  $e_q = 1/3$  quarks are relatively disfavored in  $\gamma\gamma$  collisions.

### 8. The $A$ -dependence of charm production

If gluon-fusion is the dominant source of charm production in hadron collisions then the nuclear number dependence of the cross section should reflect the  $A$ -dependence of the gluon structure function of the nucleus. Comparisons of the non-additivity of gluon and quark structure functions would provide an important discriminant of models proposed to explain the EMC effect in deep inelastic lepton-nucleus scattering.

Here I will mention briefly a new idea for explaining the enhancement of the nuclear structure functions in the low  $x$  domain measured by the EMC collaboration. First, for orientation, consider the electromagnetic contribution to the deep inelastic lepton cross section.

For small  $k^2 < R_A^{-2}$ , this contribution is coherent on the nucleus giving a non-additive contribution to the nuclear structure function per nucleon of order  $\frac{\alpha^2 Z^2}{A} F_A^2(k^2)$ , where  $k^\mu$  is the momentum transfer to the nucleus and  $F_A(k^2)$  is the nuclear form factor. Elastic kinematics implies

$$-k^2 = \frac{y^2 M_N^2 + k_\perp^2}{1-y} \quad (8.1)$$

where  $k^+ = yp_A^+ \frac{M_N}{M_A}$ . Coherence thus requires

$$x_{Bj} < y < \frac{1}{M_N R_A} \sim \frac{0.2}{A^{1/3}} \quad \text{and} \quad k_\perp^2 < \frac{1}{R_\pi^2}. \quad (8.2)$$

This type of electromagnetic contribution to the nuclear structure function has been recently discussed by Alexander, Gottsman, and Maor.<sup>30</sup> In our case we are interested in the hadronic contributions which are coherent on the nucleus, leaving it intact in the final state (see Fig. 7). Since the one-gluon exchange contribution necessarily excites the nucleus, we need to consider multigluon exchange contributions. The region of coherence in  $x_{Bj}$  is expected to be similar to that of the electromagnetic case. The  $A$ -dependence of the Pomeron coupling to the nucleus is roughly the same as that of the total cross sections ( $\sim A^{2/3}$ ). This gives a contribution to the nuclear structure

function per nucleon of order  $\frac{1}{A} (A^{2/3})^2 F_A^2(k^2) \sim A^{1/3} F_A^2(k^2)$ , i.e., an enhancement growing as  $A^{1/3}$  over a shrinking  $0 < x < 0.2A^{-1/3}$  interval.<sup>31</sup>

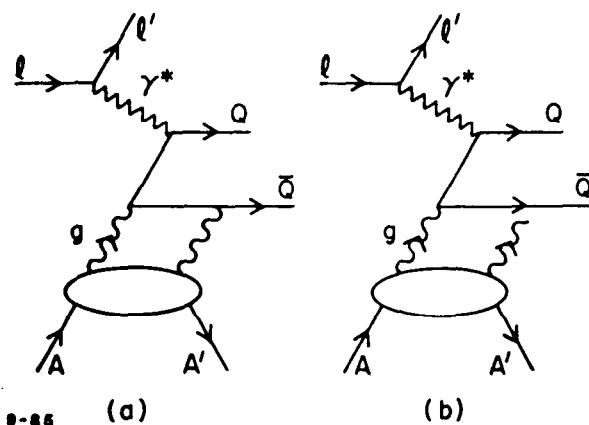


Figure 7: Coherent, nonadditive leading twist contribution to nuclear structure functions.

If the 15 to 20% enhancement seen by the EMC experiment for the iron nucleus is due to this source, then that fraction of the events in deep inelastic lepton scattering on iron should leave the nucleus intact; i.e., leave a large rapidity interval between the target and centrally produced hadrons. Because of the  $A^{1/3}$  dependence, this corresponds approximately to a 5% diffractive contribution from the proton target in the low  $x$  domain.

## 9. Pair production of heavy hadrons

One of the important testing grounds of the perturbative aspects of QCD is exclusive processes at moderate to large momentum transfer. By use of the factorization theorem for exclusive processes and evolution equations for distributions amplitudes, the leading scaling behavior and helicity dependence of form factors and hadron scattering amplitudes can be predicted.<sup>18</sup> In some cases, notably  $\gamma\gamma \rightarrow \pi^+\pi^-$  and  $K^+K^-$ , predictions for the normalization and angular behavior of the cross sections can also be made without explicit information on the nature of the bound state wavefunctions. Recent measurements of the normalization and scaling behavior are, in fact, in good agreement with the QCD predictions. In most cases, however, detailed predictions for exclusive processes require knowledge of the nonperturbative structure of the hadrons as summarized by the valence quark distribution amplitudes  $\phi_H(x_i, Q)$  of the hadrons. For example, by imposing constraints from QCD sum rules, Chernyak and Zhitnitsky<sup>33</sup> have constructed nucleon distribution amplitudes which account for the sign and normalization as well as the scaling behavior of the proton and neutron magnetic form factors at  $-q^2 > 10 \text{ GeV}^2$ .<sup>4</sup>

Exclusive pair production of heavy hadrons  $|Q_1\bar{Q}_2\rangle$ ,  $|Q_1Q_2Q_3\rangle$  consisting of higher generation quarks ( $Q_i = t, b, c$ , and possibly  $s$ ) can be reliably predicted within the framework of perturbative QCD, since the required wavefunction input is essentially determined from nonrelativistic considerations.<sup>34,35</sup> The results can be applied to  $e^+e^-$  annihilation,  $\gamma\gamma$  annihilation, and  $W$  and  $Z$  decay into higher generation pairs. The

normalization, angular dependence and helicity structure can be predicted away from threshold, allowing a detailed study of the basic elements of heavy quark hadronization.

A particularly striking feature of the QCD predictions is the existence of a zero in the form factor and  $e^+e^-$  annihilation cross section for zero-helicity hadron pair production at the specific timelike value  $q^2/4M_H^2 = m_h/2m_\ell$  where  $m_h$  and  $m_\ell$  are the heavier and lighter quark masses, respectively. This zero reflects the destructive interference between the spin-dependent and spin-independent (Coulomb exchange) couplings of the gluon in QCD. In fact, all pseudoscalar meson form factors are predicted in QCD to reverse sign from spacelike to timelike asymptotic momentum transfer because of their essentially monopole form. For  $m_h > 2m_\ell$  for factor zero occurs in the physical region.

The form factors for the heavy hadrons are normalized by the constraint that the Coulomb contribution to the form factor equals the total hadronic charge at  $q^2 = 0$ . Further, by the correspondence principle, the form factor should agree with the standard non-relativistic calculation at small momentum transfer. For zero helicity pairs these constraints are satisfied by the form<sup>34</sup>

$$F_{0,0}^M(q^2) = e_1 \frac{16\gamma^4}{(q^2 + \gamma^2)^2} \left( \frac{M_H^2}{m_2^2} \right)^2 \left( 1 - \frac{q^2}{4M_H^2} \frac{2m_2}{m_1} \right) + (1 \leftrightarrow 2). \quad (9.1)$$

At large  $q^2$  the form factor also agrees with the standard QCD prediction

$$F_{(0,0)}^M = e_1 \frac{16\pi\alpha_s f_M^2}{9q^2} \left( \frac{M_H^2}{m_2^2} \right) + (1 \leftrightarrow 2), \quad \frac{f_M}{2\sqrt{3}} = \int_0^1 dx \phi(x, Q) \quad (9.2)$$

where  $f_M = (6\gamma^3/\pi M_H)^{1/2}$  is the meson decay constant. The prediction for the  $F\bar{F}$  cross section is shown in Fig. 8 using the  $\mu^+\mu^-$  rate as reference. The basic unknown is  $\gamma^2 = v^2 m_\tau^2$  which sets the scale for capture into the wavefunction in relative transverse momentum. The same probability amplitude enters the normalization of the inclusive production of heavy hadrons in heavy quark hadronization. Although the measurements require large luminosity, the observation of the zero structure predicted by QCD would provide a unique test of the theory and its applicability to exclusive processes.

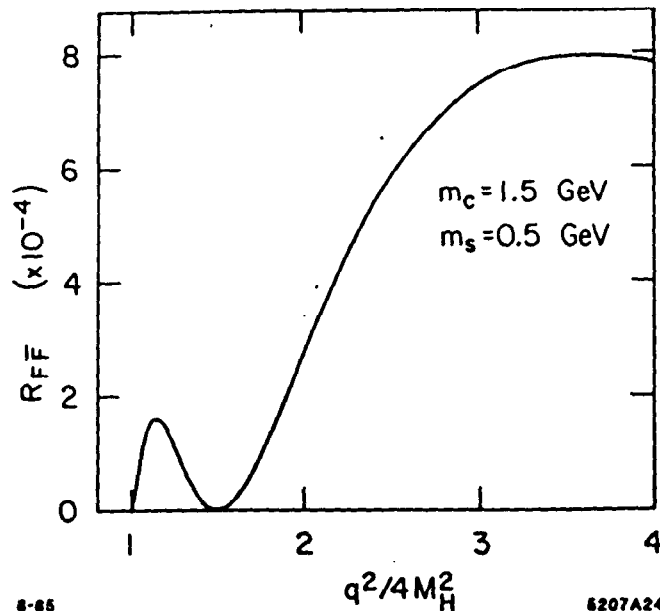


Figure 8: QCD predictions for  $\sigma(e^+e^- \rightarrow F\bar{F})/\sigma(e^+e^- \rightarrow \mu^+\mu^-)$  assuming  $\gamma = 1$ .

## 10. Conclusion

The understanding of the correct mechanisms for charm production is important not only for testing QCD, but also for providing a reliable extrapolation to the production of heavier quark states, supersymmetric hadrons, and other states containing heavy  $SU(3)$ -colored constituents. Reliable estimates of the heavy quark background to new rare processes, the background to Drell-Yan processes, possibilities for secondary beams of  $c$ ,  $b$ , and  $t$  quark hadrons, and radiation shielding considerations for new high energy, high luminosity accelerators such as the SSC depend on a clear understanding of heavy quark production processes at high energies and large  $x_L$ . The possibility of using kaon or hyperon beams to enhance heavy quark production also needs to be explored. From the theoretical point of view, a basic understanding of charm production in QCD should lead to new insights into mechanisms for quark and gluon jet hadronization, the interaction of quarks in nuclear matter, and features of hadron wavefunctions involving heavy quark constituents.

It is clearly very important that the experimental situation for charm hadroproduction be clarified. The ISR result on the magnitude,  $x_L$ -dependence and diffractive properties need to be confirmed and extended to  $SppS$  energies. A careful study of the intrinsic charm component at large  $W^2$  and  $x_B$ ; in deep inelastic muon scattering is also needed. At this point little is known on the dynamics of  $b\bar{b}$  and  $t\bar{t}$  production. The fusion subprocesses should give a good estimate of the total cross section, but the effects of prebinding distortion, intrinsic heavy particle Fock states, and the recombination with the spectrum quarks could lead to a wealth of novel effects in the forward and target or beam fragmentation regions.

### Acknowledgements

Part of this work is based on recent collaborations with J. Gunion, D. Soper, M. Soldate, A. Mueller, H. Haber, J. Collins, and C.R. Ji. Work supported by the Department of Energy, contract DE-AC03-76SF00515 and by the National Science Foundation under Grant No. PHY82-17853, supplemented by funds from NASA.

### References

1. For a review of the prediction of the fusion and other alternative models, see F. Halzen, In Proceedings of the 21st International Conference on High Energy Physics, J. de Phys. Colloq. C-3 Suppl. #12, p. 401 (1980).
2. A. Kernan and G. VanDalen, *Phys. Reports* **106**, No. 6. (1984), and references therein.
3. A critical review of the charm hadroproduction data and the problem of interpretation due to trigger biases, statistics, etc., is given by J.L. Ritchie, to appear in the Proceedings of the 1984 Summer Study on the SSC, Snowmass, Colorado (1984).
4. M. MacDermott, RAL-85-034 (1985).
5. M.E. Duffy, *et al.* WISC-EX-85-225 (1985).
6. S.F. Biagi, *et al.* *Phys. Lett.* **122B**, 455 (1983).
7. J. Gossling, DESY F21-82-01 (1982), and private communication; J. Aubert *et al.* *Nucl. Phys.* **213B**, 31 (1983). Data for the BFP experiment is only available at lower  $x_B$ , and  $Q^2$ . See Ref. 3.
8. G. Arnison, *et al.* *Phys. Lett.* **147B**, 222 (1984).
9. I.M. Dremin and V.I. Yakovlev, Levedev Institute preprint No. 141 (1984).
10. M. Basile, *et al.* *Lett. Nuovo Cimento* **30**, 487 (1981).
11. M. Aguilar-Benitez, *et al.* *Phys. Lett.* **123B**, 98 103 (1983). S. Reucroft, Proceedings of the 14th International Symposium on Multiparticle Dynamics, lake Tahoe (1983).
12. K.L. Giboni, *et al.* *Phys. Lett.* **85B**, 437 (1979).
13. J.L. Ritchie, *et al.* *Phys. Lett.* **138B**, 213 (1983).
14. D.S. Barton, *et al.* *Phys. Rev.* **D27**, 2580 (1983).
15. E. Hoffman and R. Moore, Manchester preprint M/C TH-83/11.

16. D.E. Soper, J.C. Collins, G. Sterman, OITS 292 (1985).
17. G.T. Bodwin, S.J. Brodsky, G.P. Lepage, preprint ANL-HEP-CP-85-32, and references therein.
19. S.J. Brodsky, J.F. Gunion, D.E. Soper (in preparation).
20. See, *e.g.*, A.I. Akhiezer and V.B. Berestetsky, *Quantum Electrodynamics*, Moscow (1953).
21. S.J. Brodsky, and J.F. Gunion, to be published.
22. J.D. Bjorken *Is the ccc a new deal for baryon spectroscopy?* FNAL preprint, 1985.
23. K. Hornbostel, private communication.
24. S.J. Brodsky, P. Hoyer, C. Peterson and N. Sakai, *Phys. Lett.* **93B**, 451 (1980); S. Brodsky, C. Peterson and N. Sakai, *Phys. Rev.* **D23**, 2745 (1981). G. Bertsch, S.J. Brodsky, A.S. Goldhaber and J.F. Gunion, *Phys. Rev. Lett.* **47**, 297 (1981); P.D.B. Collins and T.P. Spiller, Durham preprint DTP/84/26.
25. S.J. Brodsky, H.E. Haber and J.F. Gunion, SLAC-PUB-3300, Proceedings of the DPF Workshop on  $p\bar{p}$  Options (1984).
26. S.J. Brodsky, J.C. Collins, S.D. Ellis, J.F. Gunion, A.H. Mueller, Proceedings of the 1984 Summer Study on the SSC, Snowmass, Colorado (1984).
27. V. Barger, R.J.N. Phillips. *Phys. Rev.* **D31**, 215 (1985); G. Köpp, J.H. Kühn, P.M. Zerwas, CERN-TH 4081/1984; A. Ali, G. Ingelman, CERN-TH 4105/85.
28. A. Bassetto, M. Ciafaloni, and G. Marchesini, *Phys. Reports* **100**, 201 (1983), and references therein.
29. A.J. Mueller and P. Nason, preprint CU-TP-303 (1985).
30. G. Alexander, E. Gotsman, and U. Maor, preprint TAUP 1365-85; E. Gotsman, these proceedings.
31. S.J. Brodsky and M. Soldate (in preparation). Non-additive radiative corrections will also be discussed in this paper.
32. S.J. Brodsky and G.P. Lepage, *Phys. Rev.* **D24**, 1808 (1981); The calculation of  $\gamma\gamma \rightarrow B\bar{B}$  is given by G.R. Farrar, E. Maina, and F. Neri, RU-85-08 (1985).
33. V.L. Chernyak and A.R. Zhitnitskii, *Phys. Rept.* **112**, 173 (1984); *Nucl. Phys.* **B246**, 52 (1984).
34. S.J. Brodsky and C.R. Ji, SLAC-PUB-3756 (1985), and references therein.
35. R.R. Horgan, P.V. Landshoff, and D.M. Scott, *Phys. Lett.* **110B**, 493 (1982); F. Amiri, B.C. Harms, and Cheung-Ryong Ji, SLAC-PUB-3749 (1985).